University of Tartu

Faculty of Science and Technology

Institute of Technology

Madis Harjo

ELECTRO-CHEMO-MECHANICAL DEFORMATION STUDIES ON POLYPYRROLE COVERED GELATIN FIBER SCAFFOLDS

Masters thesis (30 EAP)

Supervisors:

Dr. Rudolf Kiefer

Dr. Martin Järvekülg

Tartu 2016

INFORMATION PAGE

Electro-chemo-mechanical deformation studies on polypyrrole covered gelatin fiber scaffolds

Polypyrrole (PPy) covered thermally cross-linked glycose-containing electrospun gelatin meshes [1] were studied as possible nontoxic and biodegradable actuators for cell growth and stimulation substrate materials. With electro-chemo-mechanical deformation (ECMD) studies it was determined that electrospinned gelatin fiber scaffolds covered with PPy/dodecylbenzenesulfonate (PPyDBS) or PPy/CF_3SO_3 (PPyTF) actuate at low voltages in range of 0.65 V to -0.5 V. Depending on the doping and polymer thickness the stress levels up to 3.5 MPa. Actuation studies were made in 0.1 M $TBAF_3SO_3$ in propylene carbonate (PC) and in Dulbecco's modified Eagle's medium (DMEM) what contained penicillin/streptomycin (PENSTREP) solution and fetal bovine serum (FBS).

Keywords: polypyrrole, gelatin fiber, electrospinning, Electro-chemo-mechanical deformation studies

CERCS codes: P250 Condensed matter: structure, thermal and mechanical properties, crystallography, phase equilibria. P260 Condensed matter: electronic structure, electrical, magnetic and optical properties, superconductors, magnetic resonance, relaxation, spectroscopy

Polüpürrooliga kaetud želatiinfiiber-mattide elektrokeemilis-mehhaaniliste deformatsioonide uuringud

Polüpürrooliga (PPy) kaetud želatiinfiibermatte uuriti kui aktuaatoreid, mis oleksid võimelised rakukasvualustena rakke mehhaaniliselt stimuleerima. Elektrokeemilis-mehhaaniliste deformatsioonide uuringutega tõestati, et fiibermatid, mis olid kaetud PPy/dodetsüülbenseensulfonaadiga (PPyDBS) ja PPy/ CF_3SO_3 (PPyTF) aktueeruvad madalatel pingetel (0.65 V kuni -0.5 V). Erinevate polümeeri paksustega ja dopeeringutega mõõtmisi läbi viies saavutati kõige kõrgemaks mehhaaniliseks pingeks 3.5 MPa. Aktuatsiooni mõõtmised viidi läbi 0.1 M $TBAF_3SO_3$ propüleenkarbonaadi lahuses ning Dulbecco Eagle meediumis, mis sisaldas ka penitsilliini ja streptomütsiini lahust (PENSTREP) ning veiselooteseerumit (FBS).

Märksõnad: polüpürrool, želatiinfiiber, elektroformeerimine, elektrokeemilis-mehhaaniliste deformatsioonide uuringud

CERCS koodid: P250 Tahke aine: struktuur, termilised ja mehaanilised omadused, kristallograafia, phase equilibria. P260 Tahke aine: elektrooniline struktuur, elektrilised magneetilised ja optilised, omadused, ülijuhtivus, magnetresonants, spektroskoopia.

TABLE OF CONTENTS

Information Page 2

Electro-chemo-mechanical deformation studies on polypyrrole covered gelatin fiber scaffolds 2

Polüpürrooliga kaetud želatiinfiiber-mattide elektrokeemilis-mehhaaniliste deformatsioonide uuringud 2

Table of Contents 4

Figures 6

Tables 7

Abbreviations 8

Introduction 9

Literature overview 10

Actuators 10

Conductive polymer actuators 12

Porous substrates for actuators 13

Pyrrole 13

PPyDBS 14

PPy/TBACF_3SO_3 (PPyTF) 14

Electrochemical synthesis 15

Electro-chemo-mechanical deformation studies 15

Cell culture medium 16

Surface resistivity measurements 17

Experiments 18

Materials and methods 18

Making fiber scaffolds 18

Fabrication of fiber scaffold 18

Electrochemical synthesis 19
PPyDBS and PPyTF synthesis onto chemically fabricated fiber scaffold 19
PPyDBS and PPyTF synthesis onto steel 20
Strain and stress measurements 21
Cell culture medium 21
PC/TF electrolyte 22
Results and analysis 23
Actuators thicknesses, surface conductivities and SEM pictures 23
Polymerization curves 25
Actuation properties of CP-film and CP-fiber scaffolds 27
PPyDBS-film and -fiber scaffolds in organic and aqueous electrolytes 28
PPyDBS samples in organic PC-TF electrolyte 28
PPyDBS samples in aqueous CCM 31
PPyTF-film and -fiber scaffolds in organic electrolytes 34
PPyTF samples in CCM 36
Isometric ECMD response at applied square wave potentials for PPyTF in 38
Comparison of PPyDBS and PPyTF samples 39
Polüpürrooliga kaetud želatiinfiiber-mattide elektrokeemilis-mehhaaniliste deformatsioonide uuringud 42
Acknowledgements 43
References 44
Lihtlitsents 47

FIGURES

Figure 1 Working principles of a) dielectric EAP: b) IEAP 11
Figure 2 Classification of artificial muscles 11
Figure 3 Schema of the linear muscle analyser 16
Figure 4 Four point probe setup 17
Figure 5 Electrochemistry cell build 20
Figure 6 PPyTF film and stainless steel plate 21
Figure 7 a) fiber scaffold without PPy coatings b) chemically coated fiber scaffold 24
Figure 8 EC synthesizsed PPyDBS and PPyTF SEM pictures 25
Figure 9 PPyDBS polymerization curves 26
Figure 10 PPy-TBACF3SO3 polymerization curves 27
Figure 11 Cyclic voltammetric measurements in PC/TBACF$_3$SO$_3$ electrolyte of PPyDBS 29
Figure 12 Square wave potentials between of PPyDBSin PC-TF 30
Figure 13 Cyclic voltammetric measurements in CCM electrolyte of PPyDBS 32
Figure 14 Square wave potentials between of PPyDBS in CCM 33
Figure 15 Cyclic voltammetric measurements in PC-TF electrolyte of PPyTF 34
Figure 16 Square wave potentials between of PPyTF in PC-TF 36
Figure 17 Cyclic voltammetric measurements in CCM of PPyTF 37
Figure 18 Square wave potentials of PPyTF and PPyDBS in CCM 38
Figure 19 Stress values of PPyDBS and PPyTF in a: PC-TF electrolyte and b: CCM 39
Figure 20 Stress values of PPyDBS and PPyTF in a: PCTF electrolyte and b: CCM 40

TABLES

Table 1 Measurements of not actuated films and fiber scaffolds 23
Table 2 Measurements of actuated films and fiber scaffolds 23

ABBREVIATIONS

APS- ammonium peroxydisulfate

CA- chronoamperometry

CCM- cell culture medium (combination of DMEM, PENSTREP and FBS)

CP- conductive polymers

CV- cyclic voltammetry

CNT-carbon nanotube

DBS – dodecylbenzenesulfonate

DMEM- Dulbecco's modified Eagle's medium

EAP- electromechanically active polymer

EC- electrochemical

ECMD- electro-chemo-mechanical deformation

FBS- fetal bovine serum

IEAP- ionic electromechanically active polymer

IL- Ionic liquid

MEG- monoethylene glycol

PC- propylene carbonate

PENSTREP- penicillin/streptomycin

PPy- polypyrrole

Py- pyrrole

SEM- scanning electron microscope

INTRODUCTION

Biomaterial science has existed for about 60 years and the concept of biomaterial has changed several times over that time. Nowadays biomaterials are considered to be biocompatible materials that interact with biological systems in a desired way. Older generation biomaterials were mostly designed to be biocompatible and inert but nowadays that idea has changed and rising trend shows that more and more materials are developed with the idea to be biocompatible, biodegradable, suitable for bioelectronics and also to be able to interact with biological systems [2].

A wide choice of laboratory apparatuses has been developed for mechanical stimulation of cell and tissue cultures. Mostly they are made of elastic materials that can be bent or stretched by machines in order to stimulate cells mechanically [3] but usually they require complex systems and expensive hardware to operate. The development of artificial muscles has created several opportunities to simplify complex systems and create new ways to advance biomaterials to a new generation.

Purpose of this work was to develop a novel material that is nontoxic, biocompatible and could actuate in aqueous solutions and at low (-1V to 1V) potentials. Other requirements were that it would not need any complex systems to operate, would also be safe for *in vitro* cell and tissue experiments and could stimulate cells and tissue.

LITERATURE OVERVIEW

Actuators

Artificial muscles are materials which describe the functionality of muscle work in comparison to natural muscles. Actuators with muscle-like structure or functionality are desirable in different fields of industries and working environments and mostly their properties are compared with mammalian muscles. Actuators mimicking natural muscles are essential in robotics, medicine, biotechnology and in many fields where properties, such as linear movement, volumetric effect, miniaturization, silent movement, biocompatibility, high power-to-weight or -volume ratios are required.

The goal for electromechanically active polymers (EAP) is to reach the efficiency and moving ability of a natural muscle. Main part of actuators functionality is that mechanical response is triggered through electrical stimuli which leads to mechanical properties change in shape or volume. Also elasticity and processability are attractive properties of EAPs.

These properties are used to construct actuators with linear, bending or twisting types of motion. EAP actuators can be used in many application areas. Advantages, such as simplicity, softness, low weight and ease of miniaturization are important for fields of prosthetics, biomimetics, implantable and wearable devices etc.

They have several advantages over other artificial muscles. They have typically flexible design, simultaneous sensing properties, inherent scalability, silent operation, potential energy harvesting ability [4, 5]. Because of the simple construction of EAPs and their key properties, they are easily scalable- including miniaturization by cutting into smaller pieces, bundling and production using micro-machinery, photolithography, dry etching and laser ablation. They are ideal candidates for microelectromechanical systems and lab-on-chip devices.

EAPs can be divided into two bigger groups based on their activation mechanism: dielectric EAPs and ionic EAPs (IEAP). The working principles of typical dielectric and ionic EAPs are illustrated in Figure 1.

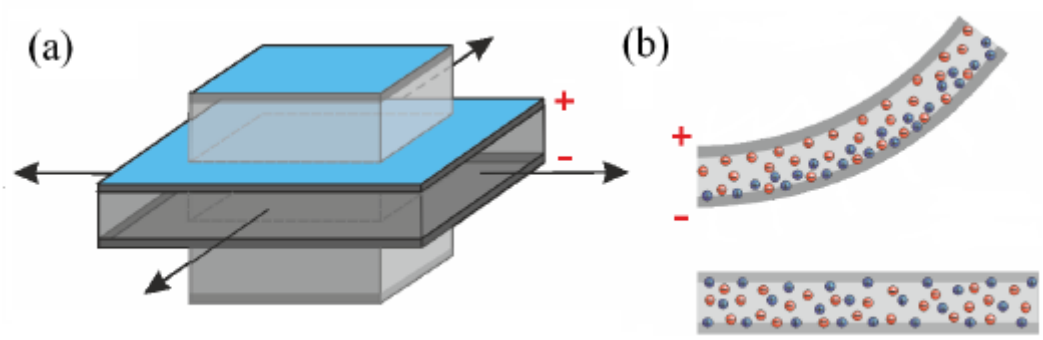

Figure 1 Working principles of a) dielectric EAP: b) IEAP [30]

In case of dielectric EAPs, the actuation is caused by various charging effects or electrostatic forces and they do not need electrolytes to function. In case of IEAPs, the electrostatic forces move around electrolyte ions that cause actuation. Examples of IEAPs include conducting polymers [6], ionic polymer metal composites [7], polymer gels [8], and carbon/based ionic actuators (e.g. carbide-derived carbon) [9]. Typical representatives of ionic EAP actuators are based on electric double layer charge transfer. Also redox processes are involved in conductive polymer (CP) actuators. By the widely accepted classification of artificial muscles (Figure 2) CP actuators belong to the ionic branch of the EAP actuators.

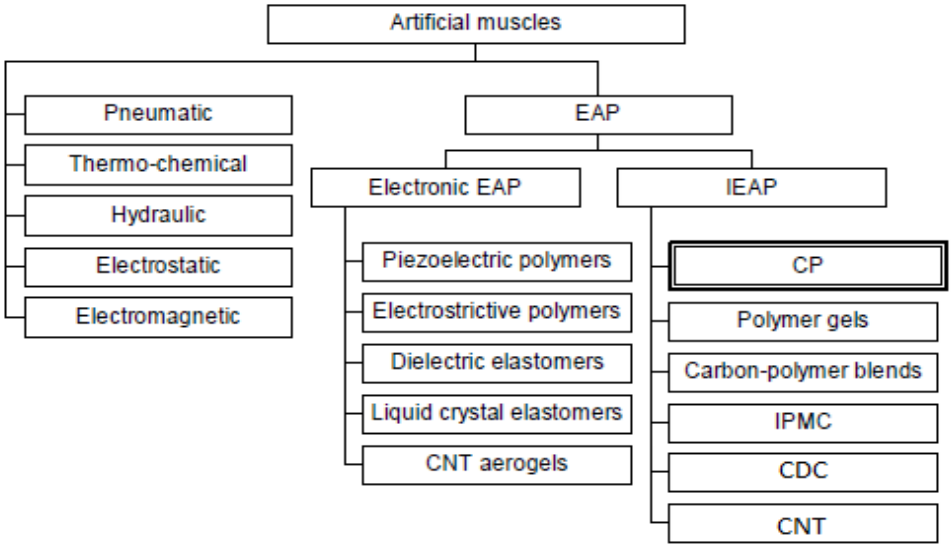

Figure 2 Classification of artificial muscles

All EAP classes have distinctive advantages and disadvantages and properties optimal for different applications. A significant difference of several EAP actuator types compared to mammalian muscles is the “catch state” property which is an ability to maintain position under constant load without energy consumption [6].

Conductive polymer actuators

CPs can be described as chemically or electro-chemo-mechanically active materials. The low voltage of 0.5V to 3V needed for actuation is making them candidates for applications, where low actuation voltages are needed.

The working principle of CP actuators usually relies on the electrochemical change by reduction or oxidation (addition or removal of electrons from polymer chains) [11,12]. Intake or ejection of ions between the polymer matrix and the associated electrolyte to balance the charge causes swelling or contraction of the polymer [30], which leads to CP volume change and can be transformed to mechanical work. Therefore, in order to function, CP actuators must have an electrolyte, a power source and at least two electrodes where at least one of them contains an active CP material.

CP actuators can be classified by a number of characteristics:

- By active CP material: PPy, PEDOT, PANI, combined from different CPs *etc*.
- By operating environment: electrolyte, air, vacuum, *etc*.
- By motion: linear, bending and twisting.
- By electrolyte: salts, dissolved in water, organic solvents or ionic liquids (IL).
- By number of layers: freestanding, bi-layer, tri-layer, *etc*.
- By membrane type: none, interpenetrated network, solid polymer gel electrolytes, porous membranes and ionomers.
- By type of dominant mobile ion: anion-active, cation-active, mixed type.
- By geometry: beam, tubular/coaxial, non-uniform.

All of the before mentioned actuator types can be combined together for scale-up. All types have their advantages and disadvantages depending on the targeted applications. In the current work we made electrolyte operated linear tri-layered actuators.

Linear actuators change their volume due to the flux of ions and usually move in linear direction. Linear actuators are usually operated in electrolyte and they require a counter electrode.

Porous substrates for actuators

Porous substrates are used as middle layers of the actuators as electrolyte storage and electronic separator layer for tri-layer air-operated bending actuators and as a mechanically supporting interlayer for in electrolyte operated linear actuators.

The introduction of electrospinning technique in synthesis of microporous substrates opens great prospects for substrate mass production and practical applications. This promising method has wide range of suitable substrates. Due to their extremely attractive potential, applications in separations, chemical sensors, membrane reactors, and catalysis, *etc.*, microporous membranes and films have been lately under large-scale investigation [16].

Thermally cross-linked glucose-gelatin electro-spun scaffolds were studied as possible substrate materials. Gelatin is a protein derived by hydrolysis from collagen. Collagen is naturally occurring protein mostly found in connective tissue. Both collagen and gelatin are considered as suitable materials for tissue engineering [1]. It was found that the addition of glucose increases cross-linking of fibrous gelatin scaffolds, which determines scaffold properties and its usability in tissue engineering. Short-term cell culture experiments indicate that thermally cross-linked gelatin-glucose scaffolds are suitable for tissue engineering applications. [1]

Pyrrole

In the current work, polypyrrole (PPy) was used as CP. It can be prepared chemically as coatings, dispersions, powders *etc*. or EC as coatings or freestanding films.

The number of different CPs is virtually unlimited, nevertheless, among many others, PPy is still one of the first discovered and the most studied CPs. PPy is researched because of good conductivity, biocompatibility (including with mammalian cells [17]), stability at ambient conditions, versatility of the synthesis methods and broad range of synthesis conditions. PPy as a CP is also attractive material for scientific research due to the low oxidation potential of the Py monomer. PPy has large variety of applications, and huge commercial potential because it is easily EC synthesizable in aqueous solutions. PPy can be polymerized at neutral pH and it retains its conductivity up to pH 10 [18].

PPyDBS

PPy doped with DBS have been studied intensely in the past 20 years. Its actuation properties are an effect of immobilized DBS^- anions during polymerization that lead to cation (with solvent molecules) incorporation at reduction [19]. Which ion leads to actuation properties of CP is still under investigation and in most cases mixed ions (cation and anion) were found during reversible redox cycles [20]. Their appearances depend on polymerization conditions, electrolyte properties, temperature and pretreatment of the PPyDBS film [21]. Recently, [22] it was found, that PPyDBS film in linear actuation can be trained starting from cation-driven actuation to anion-driven actuation by switching from organic to aqueous electrolyte. The immobilized DBS^- anions became inactive and strain in range of 3-7% was obtained [22].

In this work PPyDBS type actuators are studied in simulated body liquids to incorporate smart devices in field of medical treatment [19] and activation of STEM cells over mechanical volume change [17].

PPy/$TBACF_3SO_3$ (PPyTF)

Another type of actuator used in this thesis is PPy based actuator polymerized galvanostatically (with constant current) in propylene carbonate solution with organic electrolyte ($TBACF_3SO_3$ (TF). The solvated TBA^+ cations and solvated $CF_3SO_3^-$ anions are applied to obtain PPyTF linear actuators with strain in the range of 6-8% [23]. At potentiostatic polymerization it was discovered that due to the size and form of applied anions (CF_3SO_3) they have the tendency to be immobilized during actuation cycles, which was found relevant if switched to other electrolytes such as $TBAPF_6$ where a smaller anion PF_6^- was applied [23]. Mixed ion involvement was found as a result of this study which revealed what needs to be considered during actuation studies of CPs. Galvanostatic polymerization (constant current density) did reveal that only the anion is exchanged during reversible redox cycles when applied in aqueous $NaPF_6$ electrolytes [24]. Therefore the polymerization method is another important parameter to consider in view of cation-driven, mixed ion-driven or anion-driven actuators.

Electrochemical synthesis

Usually EC synthesis is preferred instead of chemical synthesis due to the higher conductivity of the resulting material, reproducibility and more precise control over the synthesis rate and deposition area. EC synthesis is carried out by the oxidation on the anode of the EC cell. Doping with the electrolyte anions occurs during electro-polymerization.

Galvanostatic (constant current), potentiostatic (constant potential) and dynamic methods like potentio-dynamic; sequential polymerization, *etc.* can be used as EC polymerization methods. The amount of the synthesized polymer is generally determined by the synthesis charge where Q_s is the synthesis charge, i(t) is the synthesis current and t is time:

$$Q_s = \int i(t)dt$$

Equation for synthesis charge

Properties, such as the structure, conductivity, elasticity etc. depend on a number of synthesis conditions, such as synthesis temperature, synthesis duration, deposition rate, substrate, etc. It is widely agreed that in order to obtain homogeneous, flexible and well conducting films, synthesis should be done at low temperatures, at low deposition rate and high concentration of monomer [25] and the supporting electrolyte [26].

Electro-chemo-mechanical deformation studies

This chapter describes the particular device used for force and strain measurements (Figure 3). The sample is attached between two clamps and the upper clamp is attached to a force sensor. The lower clamp is static and is fixed to the frame of the machine. Due to this setup cyclic voltamperometry, chronopotentiometry and chronoamperometry can be measured. While the sample actuates the force sensor maintains constant force in order to measure strain.

Three electrode measurements were carried out using the following setup: fiber was immersed into electrolyte in a cell with a Pt-sheet counter electrode and an Ag/AgCl (3M KCl) reference electrode. The initial length of the fiber between the clamps was 1 mm. The force changes and the applied electrical signal were measured in real time.

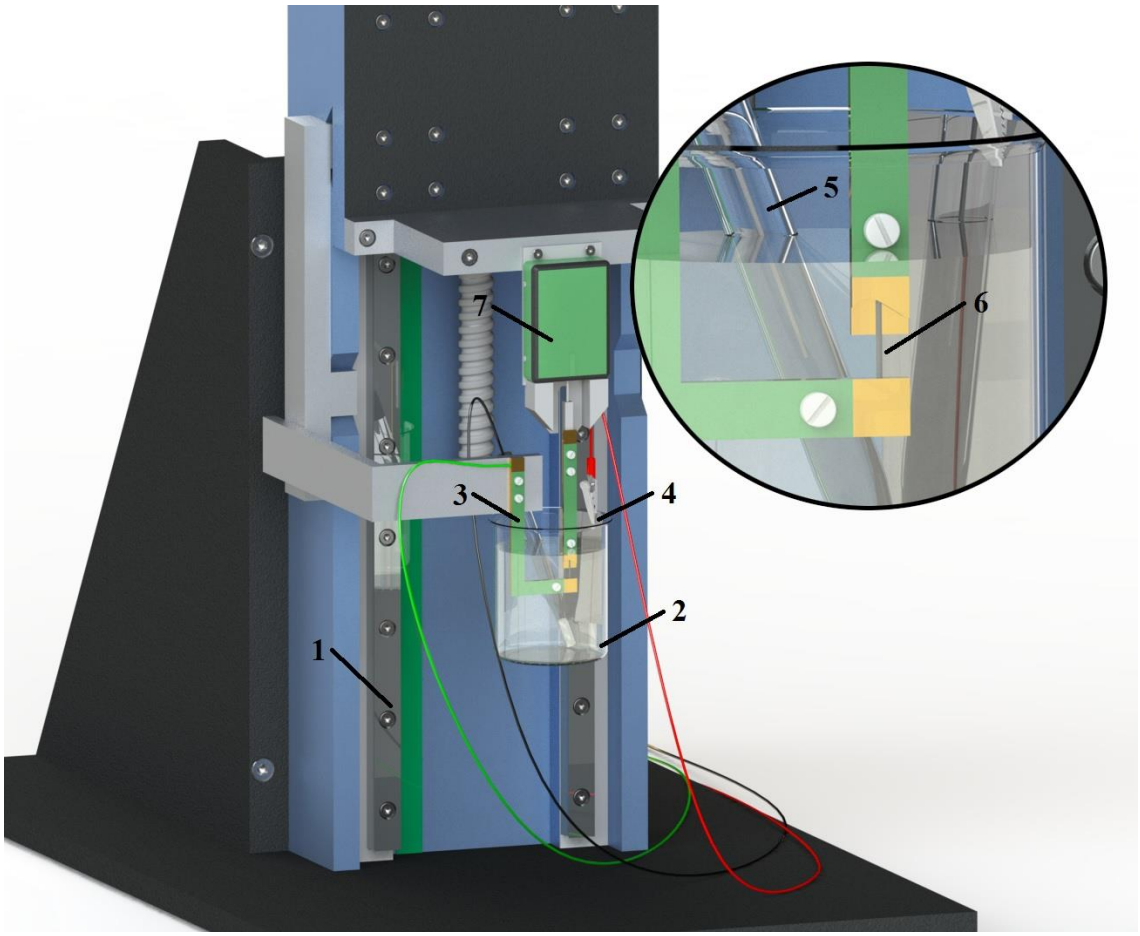

Figure 3 Schema of the linear muscle analyser with a force sensor. Precision stage (1), beaker with electrolyte (2), working electrode (3), Pt-sheet counter electrode (4), Ag/AgCl reference electrode (5), sample (6), force sensor (7) (Picture author: Margo Plaado) [22]

Cell culture medium

Cell culture medium (CCM) is a solution or gel designed to support cell growth. Since one of the purposes is to use developed material as cell culture substrate then we used Dulbecco's modified Eagle's medium (DMEM) with glycose content of 4,5g/l what contained penicillin/streptomycin (PENSTREP) solution and fetal bovine serum (FBS) as one of the electrolytes. Per 500 ml of DMEM 56ml of FBS and 4ml of PENSTREP was used.

DMEM is designed to preserve and maintain growth of a broad spectrum of mammalian cells. It mostly consists of water and different salts that are soluble in water. It is stored at temperatures 2 to 8 ˚C.

Streptomycin with penicillin is used in a standard antibiotic solution to prevent bacterial infection in cell culture. It consists of 97% of water, 0.9% of NaCl, 1% of penicillin and 1% of streptomycin sulphate. PENSTREP is usually stored frozen.

FBS is the most widely used *in vitro* cell culture serum. FBS comes from the blood drawn from bovine fetus. It is a blood fraction remaining after blood coagulation which is after collection purified from red blood cells. FBS is also usually stored frozen.

Surface resistivity measurements

Conductivity is one of the most important characteristics of conductive polymer. The four point probe was applied to measure surface resistivity (**Ω**/sq**)**. Four point probes setup is shown on Figure 4. Constant current is passed through outer contacts and potential is measured with inner contacts. Spaces between contacts are the same.

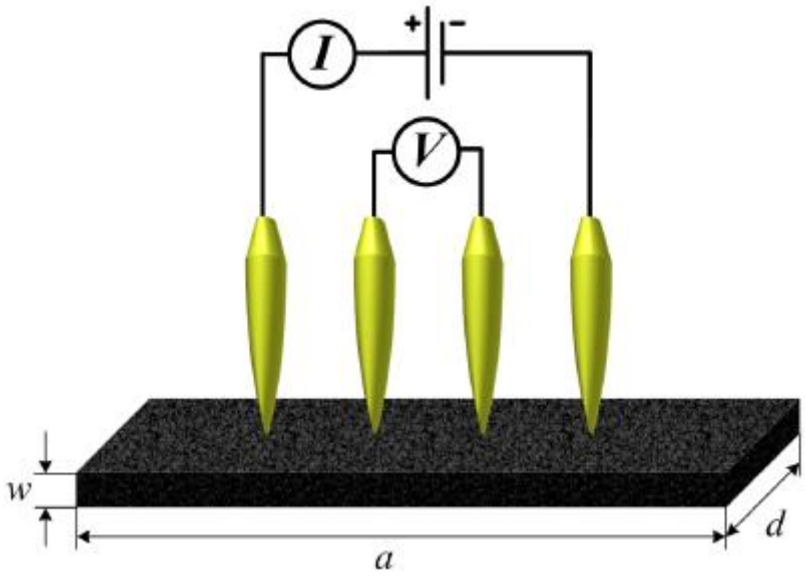

Figure 4 Four point probe setup [30]

Conductivity was calculated with equation:

$$\sigma = \frac{1}{R * w}$$

Where σ is the electric conductivity, R is surface resistivity (**Ω**/sq**)**.and w is material thickness (μm).

EXPERIMENTS

Materials and methods

Sodium dodecylbenzenesulfonate (NaDBS, 99%), propylene carbonate (PC, 99%), tetrabutylammonium trifluoromethanesulfonate (TBACF3SO3, 99%), ethan-1,2-diol (ethylene glycol, EG, 97%), tetramethylammonium chloride (TMACl, 99%) and ammonium persulfate (?) were obtained from Sigma-Aldrich and used as supplied. Pyrrole (Py, 99%, Sigma-Aldrich) was distilled and stored at -20 °C prior to use. Gelatin type A from porcine skin D-(+)-glucose (99.5%) and glacial acetic acid (99%) were also purchased from Sigma-Aldrich.

Making fiber scaffolds

Glucose and type A gelatin from porcine skin was used to prepare solution for electrospinning. Glucose was mixed with gelatin at ratio of 1/10. The mixture was dissolved in 10M acidic acid at room temperature during vigorous stirring on magnetic stirrer [1].

Fibrous scaffolds were prepared by electrospinning under following condition 5 ml syringe containing gelatin solution was pumped at speeds of 5-7µl/min at 17,5kV. New Era Pump Systems NE-511 was used as syringe pump and Heinzinger LNC 3000 for high voltage power supply. Aluminium foil was used as grounded target and it was placed 14.5 cm away from syringe needle tip. Fibrous scaffolds were then removed from the foil and stored in petri dishes until thermal treatment.

Cross-linking was carried out by placing fibrous scaffolds in an oven for 3 hours. In order to avoid gelatin degradation and to ensure proper cross-linking, fiber scaffolds were put in the oven at 175 °C [1]. Scaffold structure and fiber morphology was examined by scanning electron microscope (SEM) (Figure 7).

Fabrication of fiber scaffold

To obtain a conductive layer on to fiber scaffolds PPy was oxidized chemically [27]. Common method for the chemical synthesis is mixing of monomer and oxidant in a solution. The chemical synthesis process is less controllable and has lower yield when used for surface coating in solutions [27]. In addition, the CP layer has low quality and the thickness of CP is difficult to reproduce. Due to gelatin-glycose cross-linked fiber scaffold was not conductive and therefore not usable for EC synthesis, it needed to be covered chemically with PPy to make it conductive for EC synthesis.

Chemical PPy deposition

In this experiment fiber scaffolds were coated with PPy polymer using APS (0.075 M) and NaDBS 0.01M aqueous solution. 2M pyrrole in 40% ethanol was applied as monomer solution.

Cross-linked fiber scaffold was first put into purified water and then raised into monomer solution where it was gently stirred about 30 seconds. After that fiber scaffold was raised into APS/NaDBS aqueous solution where it was kept around 20 seconds. After 20 seconds it was put into ethanol solution where monomer was washed off and after that again into purified water where excess APS and NaDBS was washed off. This procedure was repeated 4 times until thicker polymer coating was achieved. After that it was stored in ethanol or dried using supercritical point extraction with CO_2 and kept in petri dishes.

Electrochemical synthesis

For the most part EC synthesis is preferred to chemical synthesis due to the higher conductivity of the resulting material. EC synthesized films are chemically and mechanically stable and alike and also often biocompatible. Therefore EC synthesis was used to produce final layer of polymer. Also PPyDBS and PPyTF linear films were synthesized on same polymerization condition for the reference on stainless steel, where the films could be peeled off.

PPyDBS and PPyTF synthesis onto chemically fabricated fiber scaffold

For PPy/DBS synthesis 0.2M NaDBS and 0.2M Pyrrole monoethyleneglycol (MEG)/water solution was used. MEG and purified water balance was 1 to 1. Synthesis temperature was -20˚C and synthesis times were 20,000 s and 40,000 s. Synthesis took place at constant current of 0.1mA/cm^2.

For PPyTF synthesis 0.1M Pyrrole and 0.1M $TBAF_3SO_3$ propylene carbonate solution was used. Synthesis temperature was -20 C and synthesis time was 40,000 s. Synthesis took place at constant current of 0.1mA/cm^2.

EC synthesis of the linear actuator was carried out in a two electrode cell (Figure 5) with a stainless steel fabric as counter electrode and chemically coated fiber scaffold as working electrode.

After polymerization the coated fiber scaffolds were washed with ethanol and water and stored in ethanol or dried using supercritical point extractor and CO_2. The edges of the synthesized

actuator were trimmed and 10x2 mm samples were cut from the remaining piece for strain and stress measurements.

PPyDBS and PPyTF synthesis onto steel

PPyDBS and PPyTF films were synthesized on 3x3 cm steel plate. Solutions and the synthesis conditions were same as for the previously EC coated fiber scaffolds.

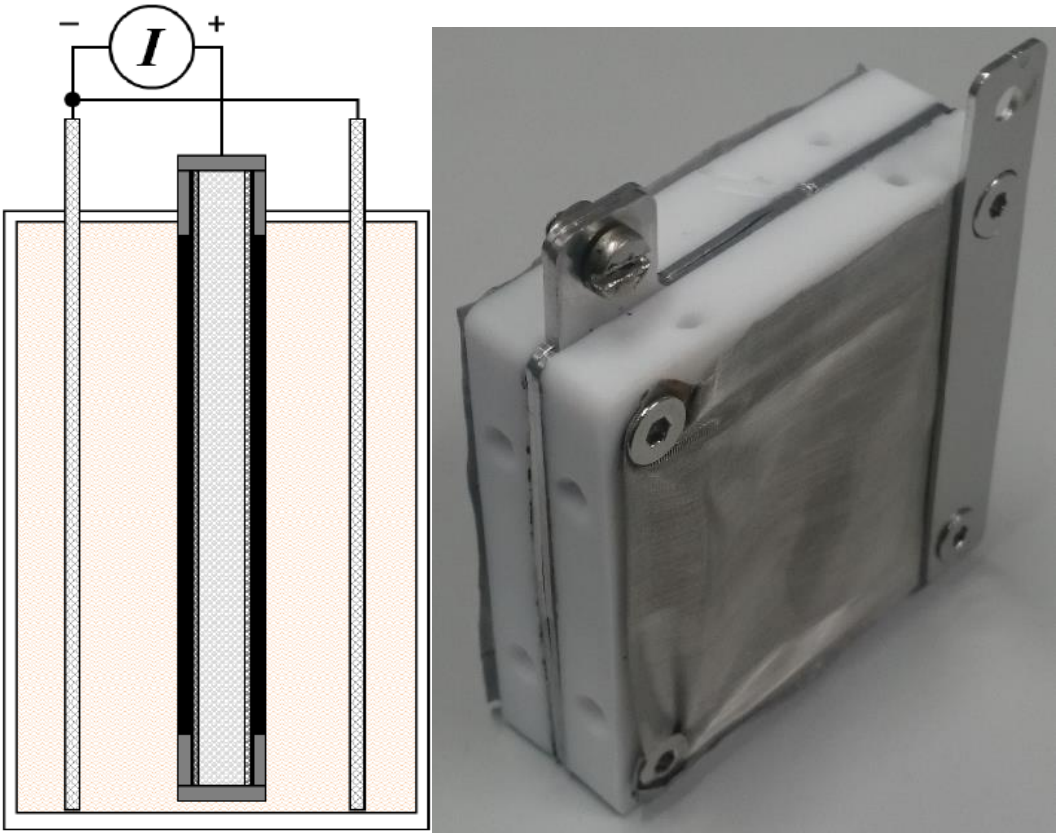

Figure 5 Left: Electrochemistry cell build [30], Right: photo of built EC cell

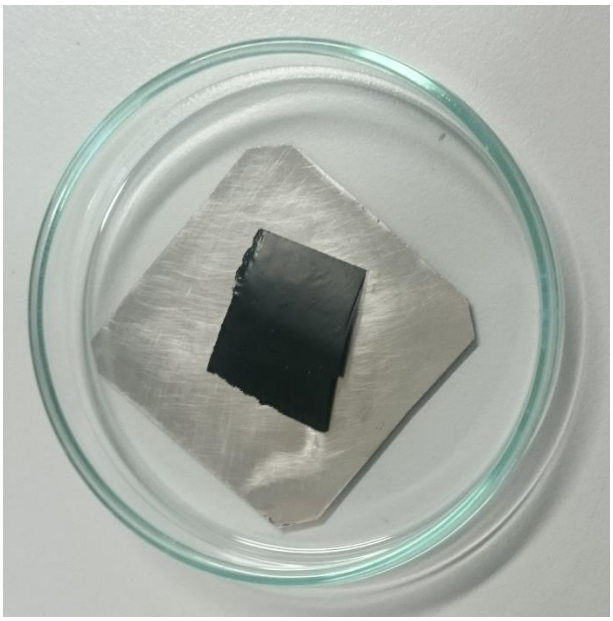

Figure 6 PPyTF film and stainless steel plate

Strain and stress measurements

Strain and stress measurements were carried out with earlier mentioned machine. 10x2 mm pieces were cut from previously polymer coated scaffolds and films and attached to the machine. Cell culture medium including DMEM, PENSTREP and FBS was used as one electrolyte. For the second electrolyte 0.1M PC/$TBAF_3SO_3$ was applied. None of the samples were measured in both electrolytes. To assure that no overoxidation takes place the actuation studies were performed under steady state condition (charging/discharging) in balance for all electrolytes and CP films.

Cell culture medium

For chronoamperometry measurements (square wave potentials) the potential range of 0.2V to -1.2V was applied at different frequencies:

- 0.05 Hz for 5 cycles
- 0.025 Hz for 5 cycles
- 0.01 Hz for 3 cycles
- 0.005 Hz for 3 cycles
- 0.0025 Hz seconds for 3 cycles

For cyclic voltammetry the potential range of 0.2V to -1.2V was applied with scan rate of 5mV/s for 3 cycles.

PC/TF electrolyte

For chronoamperometry measurements (square wave potentials) the potential range of 0.45V to -0.65V was applied at different frequencies:

- 0.05 Hz for 5 cycles
- 0.025 Hz for 5 cycles
- 0.01 Hz for 3 cycles
- 0.005 Hz for 3 cycles
- 0.0025 Hz seconds for 3 cycles

For cyclic voltammetry the potential range of 0.45V to -0.65V was applied with scan rate of 5mV/s for 3 cycles.

RESULTS AND ANALYSIS

The actuators were characterized by measuring thickness, surface conductivity, cyclic voltammetry and chronoamperometry.

Actuators thicknesses, surface conductivities and SEM pictures

Tabel 1 Measurements of not actuated films and fiber scaffolds

Polymer	Polymerization time (h)	Thickness (µm)	Surface resistivity (Ω/sqare)	Conductivity (S/m)
Crosslinked Fiber	-	16	-	-
Chemically coated fiber	-	48	-	-
PPyDBS fiber	5,55	95	123,62	85,15
PPyDBS fiber	11,11	125	34,06	234,88
PPyTF fiber	11,11	136	7,38	996,33
PPyDBS film	11,11	20	1,78	28089,89
PPyTF film	11,11	20	11,48	4355,40

Tabel 2 Measurements of actuated films and fiber scaffolds

Polymer	Polymerization time (h)	Activation electrolyte	Thickness (µm)	Surface resistivity (Ω/sqare)	Conductivity (S/m)
PPyDBS fiber	5,55	PC/TF	92	77,75	139,8
PPyDBS fiber	11,11	PC/TF	123	52,25	155,6
PPyDBS fiber	5,55	CCM	85	252,9	46,52
PPyDBS fiber	11,11	CCM	114	414,6	21,16
PPyTF fiber	11,11	CCM	109	296,35	30,96
PPyTF fiber	11,11	PC/TF	118	209,48	40,46
PPyDBS film	11,11	CCM	20	96,48	518,24
PPyDBS film	5,55	PC/TF	20	129,75	385,37
PPyTF film	11,11	CCM	20	295,35	169,29
PPyTF film	5,55	PC/TF	20	103,8	481,7

There is a trend that linear films contain lower resistivity while those on fiber increase in resistivity. The reason for that is because stainless steel has a better surface conductivity than chemically coated PPy fiber Tabel 1. Therefore the deposition of PPy on the fiber leads to

rougher and less conductive PPy network because of the rough surface of the PPy chemical coating. It can also be seen comparing Figure 8a and Figure 8c where SEM analysis shows that due to better conductivity of stainless steel plate the polymer layer on Figure 8c is more uniform than on Figure 8a which was first covered chemically and then electrochemically with PPy.

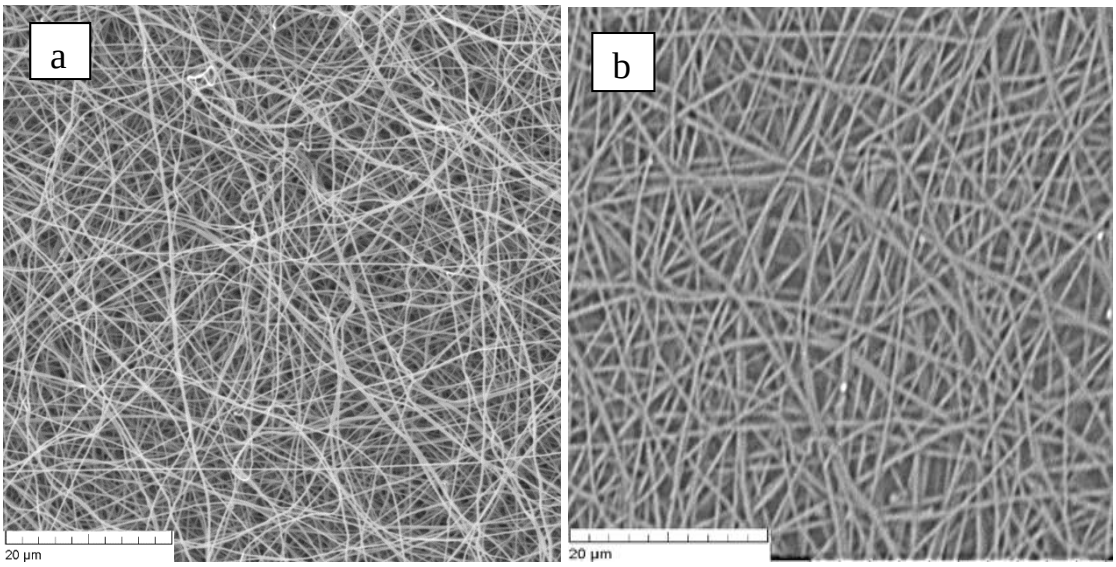

Figure 7 a) fiber scaffold without coatings b) chemically coated fiber scaffold

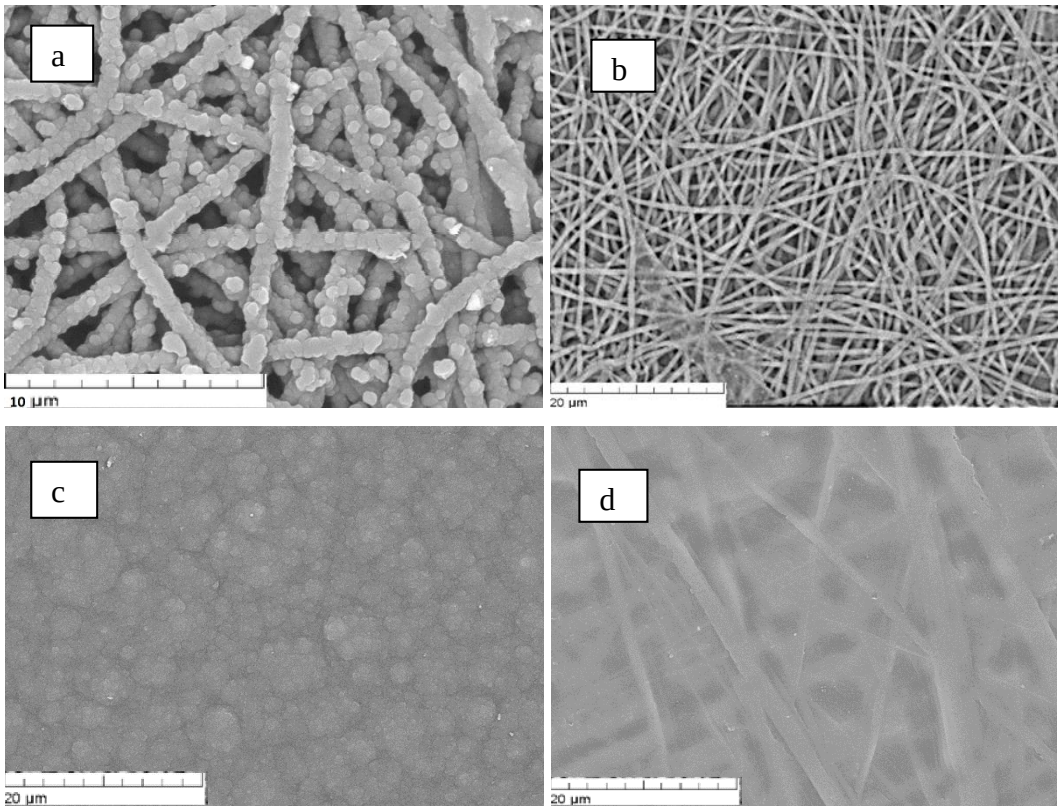

Figure 8 a) EC synthesizsed PPyDBS fiber scaffold with synthesization time of 11,11h at constant current of 0.1mA/cm^2 and temperature of -20 ˚C, b) synthesizsed PPyTF fiber scaffold with synthesization time of 11,11h at constant current of 0.1mA/cm^2 and temperature of -20 ˚C, c) synthesizsed PPyDBS film with synthesization time of 11,11h at constant current of 0.1mA/cm2 and temperature of -20 ˚C, d) synthesizsed PPyTF film with synthesization time of 11,11h at constant current of 0.1mA/cm2 and temperature of -20 ˚C

synthesizsed PPyTF film with synthesization time of 11,11h at constant current of 0.1mA/cm2 and temperature of -20 ˚C

From Figure 7b, Figure 8a and b can be seen that PPy chemical and electrochemical synthesis has not covered or closed heat treated cross-linked fiber scaffold pores (Figure 7a) and PPy has been deposited only on fibers and therefore making it good attachment surface for different mammalian cells.

Polymerization curves

To assure slow deposition of CP on conductive substrate the polymerization temperature of -20^{o}C was applied in a two electrode cell (Figure 5) with stainless steel mesh counter and reference electrode and stainless steel plate working electrode for the free standing film and the

fiber web coated with PPy (chemically) for the PPyDBS-fiber samples. Galvanostatic polymerization (potential time curves) at applied constant current for PPyDBS type is shown at Figure 9.

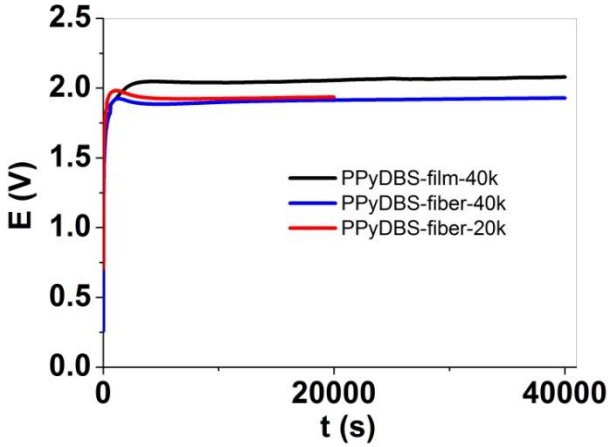

Figure 9 PPyDBS polymerization curves at applied constant current of 1.8 mA (0.1 mA/cm2, area of working electrode 18 cm2) in MEG/MilliQ (50:50 wt %) in a two electrode cell

For all samples the deposition of PPyDBS on working electrode are showing similar deposition potential in the range of 1.98 -2.06V with little decrease of 0.1V at the end of the polymerization. The different time of the polymerization for the PPyDBS-fiber-20k scaffold was applied to obtain different thickness (Tabel 1) of PPyDBS deposition, which was for PPyDBS-fiber 20k in the range of 23µm each side and for PPyDBS-fiber-40k 38µm on each side. The PPyDBS film thickness was 20µm and reflecting in higher conductivity in comparison to PPyDBS-fibers (Tabel 1). The polymerization curves for PPyTF film and fiber are presented in Figure 10.

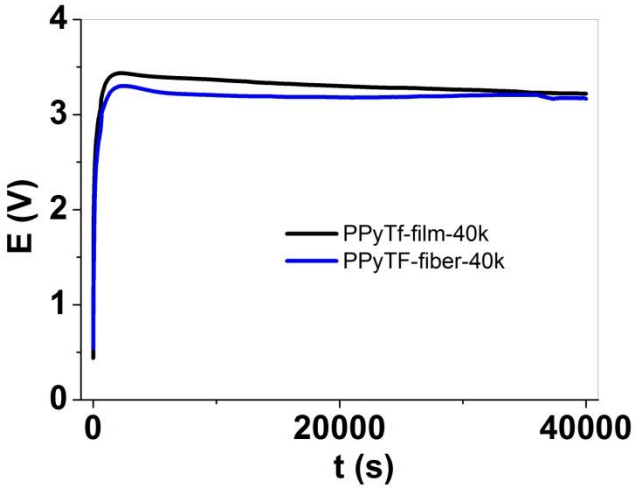

Figure 10 PPy-TBACF3SO3 (PPy-TF) polymerization curves (potential time curves) at constant current of 1.8 mA in 0.1 M TBACF3SO3 propylene carbonate electrolyte with 0.1 M pyrrole in a 2 electrode cell set up at -20 ˚C, time duration of 40,000s. The stainless steel mesh was applied as counter and reference electrode and for the PPyTF film a stainless steel sheet was applied as working electrode. In case of PPyTF-fiber-40k the PPy (chemically) coated sample was used as the working electrode

PPyTF is polymerized galvanostatically on same constant current range, temperature and polymerization cell set up like PPyDBS. The solvent applied is propylene carbonate with 0.1M $TBACF_3SO_3$ electrolyte. The deposition rate revealed (Figure 10) that the potential time curves (decrease of potential from 3.4V to 3.2V after 40,000s) for PPyTF film (thickness 20µm) and PPyTF-fiber (thickness of PPyTF 44µm each side) is in same range. The resistivity of the PPyTF film was 11.48Ω/sq which is lower in comparison to the PPyTF-fiber-40k with similar explanation given for PPyDBS-fiber-40k sample.

Actuation properties of CP-film and CP-fiber scaffolds

The samples of CP films and fiber scaffolds are immersed in actuation electrolyte solution. Isometric ECMD measurements of the samples are performed to evaluate the stress changes at applied potential with main goal to stimulate cells under mechanical movement; the stress is the most important property, rather than the strain. Cyclic voltammetric (scanrate of 5mV/s) and square wave potential measurements (frequency of 0.0025Hz) for the CP samples (PPyDBS and PPyTF) in PC-TF and CCM actuation solutions are presented in next sections. To assure that no over-oxidation and over-reduction takes place, steady state conditions were applied, which means that charging/discharging is in equilibrium [28] that can be observed if the charge

density potential curves showing a closed circle at different scan rates of cyclic voltammetric measurements.

PPyDBS-film and -fiber scaffolds in organic and aqueous electrolytes

PPyDBS samples in organic PC-TF electrolyte

Isometric ECMD response under cyclic voltammetric measurements

After EC polymerization in NaDBS with monomer (pyrrole) solution, the samples (PPyDBS-film-40ks, PPyDBS-fiber-20ks and 40ks) are immersed into PC-TF and fixed between static clamp and force sensor. To assure that the PPyDBS samples have enough time to adapt to new electrolyte (from aqueous to organic) the stretched samples were kept in PC-TF several hours before the isometric ECMD measurement was started. Steady state conditions for PPyDBS samples in organic electrolyte were established in voltage range of 0.45V to -0.65V. The results for the cyclic voltammetric measurements (scan rate of 5 mV/s) are presented in Figure 11.

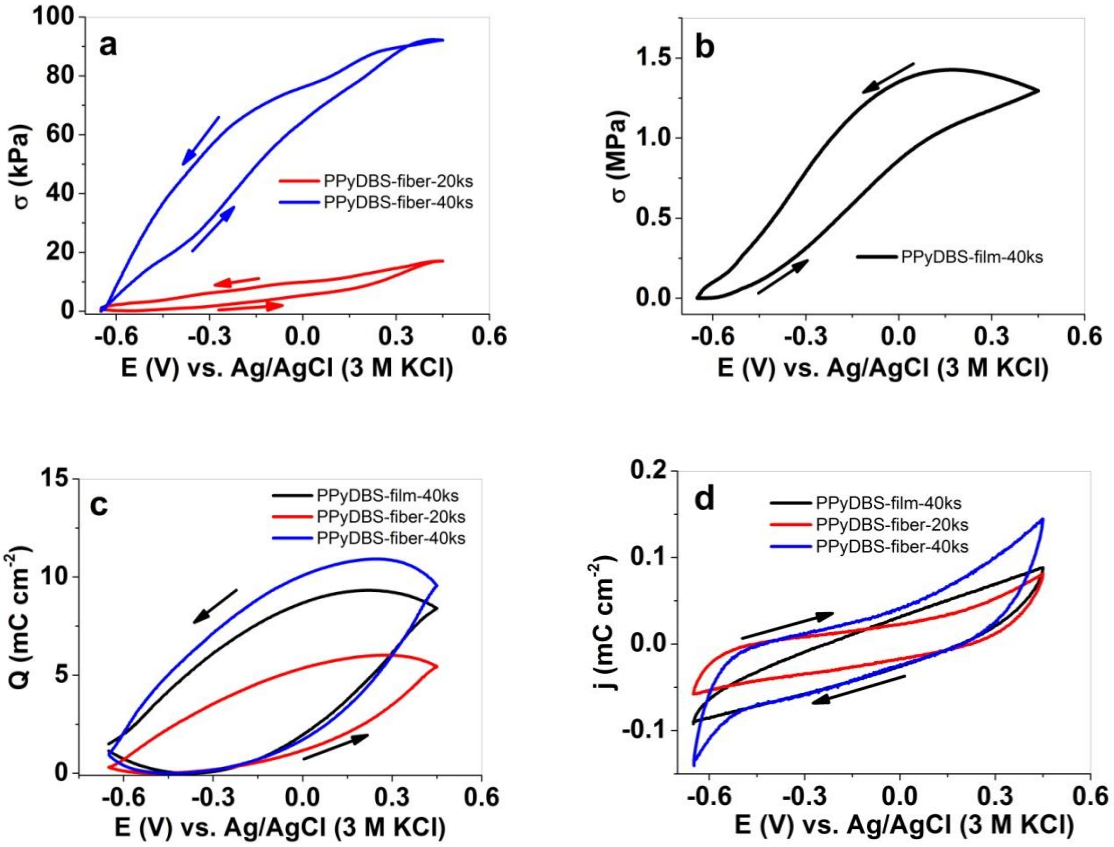

Figure 11 Cyclic voltammetric measurements (5 mV/s, third cycle) under isometric ECMD control in PC/TBACF$_3$SO$_3$ electrolyte of a: stress σ (kPa) vs potential curve of PPyDBS-fiber-scaffold-20ks (red) and 40ks (blue), b: stress σ (MPa) vs potential curve of PPyDBS-film (black), c: charge density Q vs potential curves of PPyDBS-fiber scaffolds (red, 20ks; blue 40ks) and PPyDBS-film (black) and d: current density j vs. potential curves of PPyDBS samples

Figure 11 shows the actuation properties of PPyDBS film and fiber scaffolds (20ks and 40ks) in PC-TF electrolyte. The maximum expansion observed in Figure 11a and Figure 11b shows that from -0.65V to 0.45V the increase of strain shows a contraction of the film (in general strain measurement would show a decrease in strain). The reason for that relies in the force measurement set up, where a constant length of 1 mm with weight (mg) is applied that leads to force change if the PPyDBS sample is reduced and the cation moves in (expansion from 0.45 to -0.65) at Figure 11a and Figure 11b. Keeping in mind how to analyze the measurements, cation-driven actuation of PPyDBS samples are observed in this electrolyte with expansion at reduction. PPyDBS-fiber-20ks is in the range of 17kPa and PPyDBS-fiber-40ks with 5.4 times higher stress (92 kPa). The PPyDBS-film-40ks shows stress in the range of 1.3MPa that can be explained by the thinner film thickness of 20 µm and no rigid parts between it in case for the fiber scaffolds with modulus in the range of 100 MPa [29]. The charge density of the PPyDBS

samples (Figure 11c) reveals that all systems are in steady state with double charge densities (mC cm^{-2}) of 10mC cm^{-2} for PPyDBS-fiber-40ks compared to the PPyDBS-fiber-20ks (5mC cm^{-2}) and PPyDBS-film-40ks with 8mC cm^{-2}. The reason for better charge density for PPyDBS-film-40ks relies on the nature of the free standing CP film with faster charge accumulation between PPyDBS-film electrode electrolyte interface. The current density curves (CV shapes) at Figure 11d are showing that higher current density of PPyDBS-fiber-40k takes place because of higher deposition rate of PPyDBS. That is also reflected in the thickness and resistivity given in Tabel 1 of the different samples.

Isometric ECMD response at applied square wave potentials for PPyDBS in PC-TF

Chronoamperometric measurements are showing square wave potential steps at frequency of 0.0025Hz between 0.45V to -0.65V for the samples. The stress values at applied frequency of 0.0025Hz – 0.1Hz are shown in response to the obtained stress values. The isometric ECMD measurements with correlated current density are presented in Figure 12.

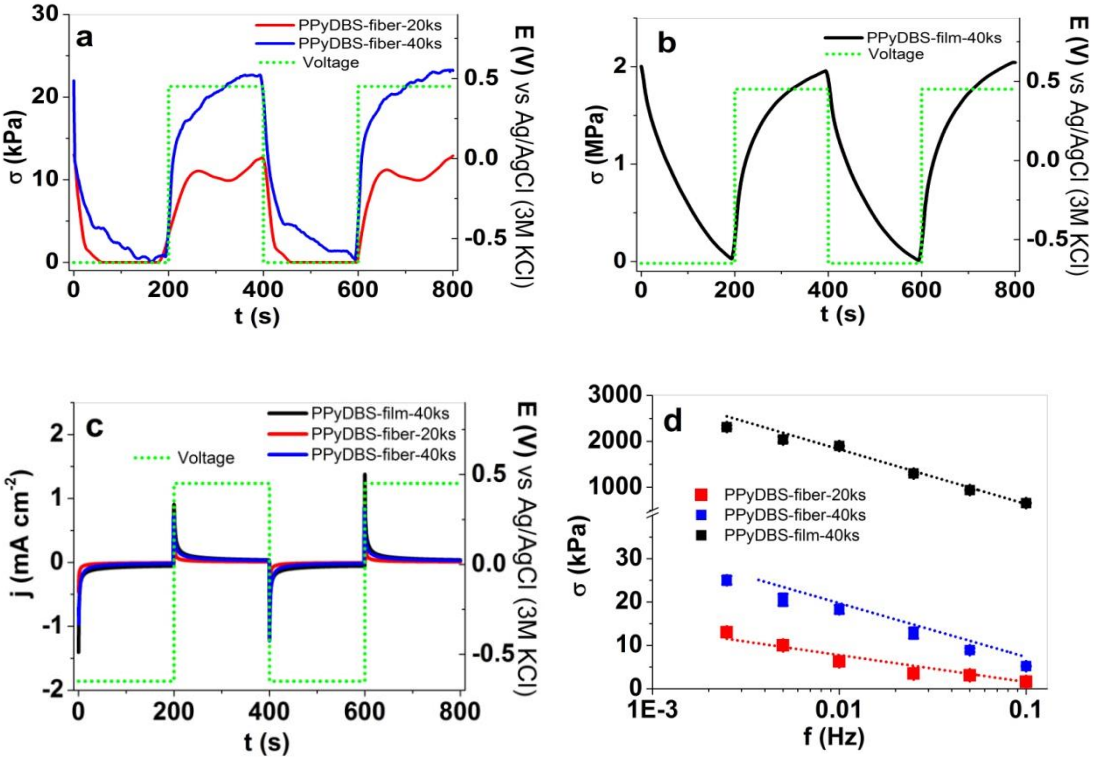

Figure 12 Square wave potentials between 0.45V to -0.65V (dotted green curve of voltage) at applied frequency of 0.0025Hz (cycle 2-3) of PPyDBS-film-40ks (black), PPyDBS-fiber-20ks (red) and PPyDBS-fiber-40ks (blue) in PC-TF solution in 3 electrode cell with counter Pt sheet electrode, Ag/AgCl (3M KCl) reference electrode and the sample (1mm length constant) as working electrode. a: stress time curves of PPyDBS-fiber (40ks and 20ks), b: stress time curves of PPyDBS-film-40ks, c: current density time curve of all

applied samples and d: stress σ (middle value with standard regression and linear fit) vs frequency (0.0025Hz -0.1Hz) of all samples

The stress time curve for cycle 2-3 (Figure 12a, b) reveals cation-dominated actuation with expected low stress for PPyDBS-fiber-20ks in the range of 12kPa and nearly double amount of 23kPa for PPyDBS-fiber-40ks. The PPyDBS-film-40ks (Figure 12b) shows stress in the range of 2MPa. The stress dependency of applied frequency (Figure 12d) are revealing nearly linear behavior for all samples with decreasing stress at increasing frequency. It needs to be noticed that for the PPyDBS film at 0.1Hz a stress above 500kPa was found, which shows the possible application of such type in microactuators or robotic devices.

PPyDBS samples in aqueous CCM

Isometric ECMD response under cyclic voltammetric measurements

Steady state condition for PPyDBS fiber scaffolds (20ks and 40ks) was established in the potential range of 0.2V to -1.2V. Figure 13 shows the stress potential curves, charge density potential curves and current density potential (CV) curves at applied scan rates of 5mV/s.

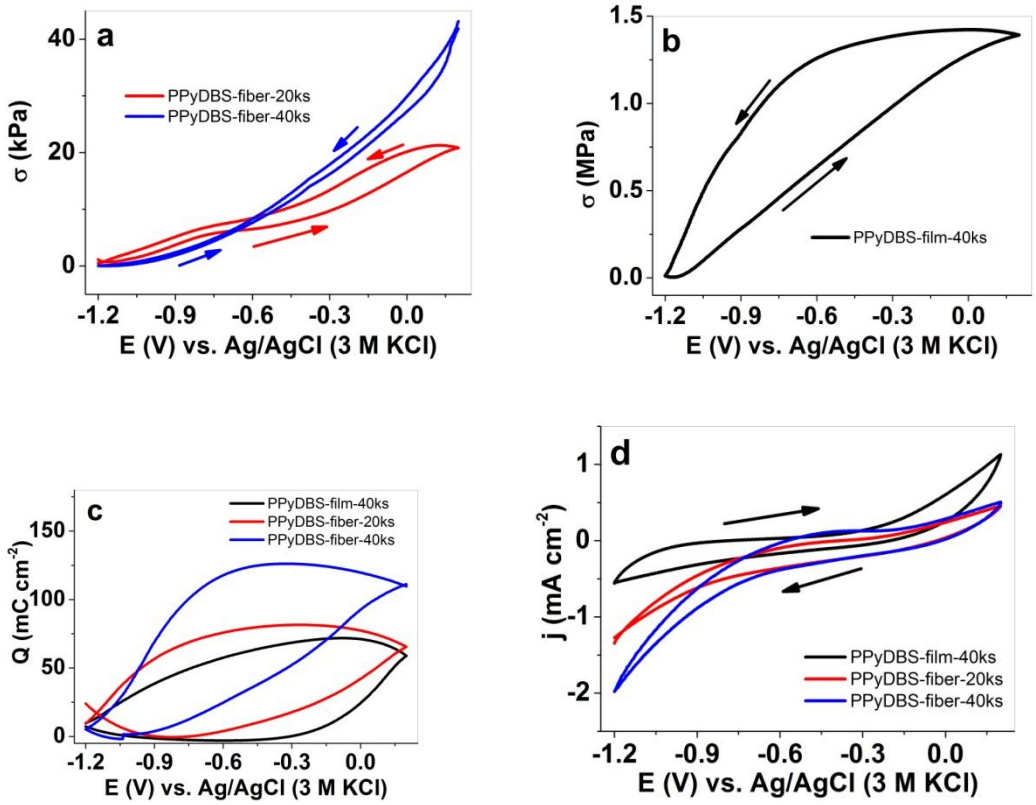

Figure 13 Cyclic voltammetric measurements (5mV/s, third cycle) under isometric ECMD control in CCM electrolyte of a: stress σ (kPa) potential curve of PPyDBS fiber scaffold 20ks (red) and 40ks (blue), b: stress σ (MPa) potential curve of PPyDBS film (black), c: charge density Q potential curves of PPyDBS fiber scaffolds (red, 20ks; blue 40 ks) and PPyDBS film (black) and d: current density j potential curves of PPyDBS samples

The PPyDBS-fiber-20k shows stress in the range of 20kPa (Figure 13a). The PPyDBS-fiber-40k has a higher amount of PPyDBS that result in higher stress in range of 40kPa (Figure 13a). It needs to be noticed that the stiffness (~100 MPa [29]) of the fiber scaffold effecting the stress extent. PPyDBS free standing film (Figure 13b) shows stress in the range of 1.4MPa (35 times higher than the PPyDBS-fiber-40ks). The reasons for higher stress relate to lower thickness of 20µm of the PPyDBS-film-40ks and expected faster cation incorporation at charging/discharging at the interface of the free standing film. If charging/discharging in balance the charge density time curves showing a closed loop which is to be found for all studied samples (Figure 13c). The charging/discharging properties for PPyDBS-fiber 40ks are in the range of 120mC/cm^2 and 70mC/cm^2 for PPyDBS-fiber-20ks. To investigate actuation properties at square wave potentials Figure 14 shows the related stress time and current density time curves at specific applied frequency of 0.0025Hz and stress changes correlated to frequencies between 0.0025Hz to 0.1Hz.

Isometric ECMD response at applied square wave potentials for PPyDBS in CCM

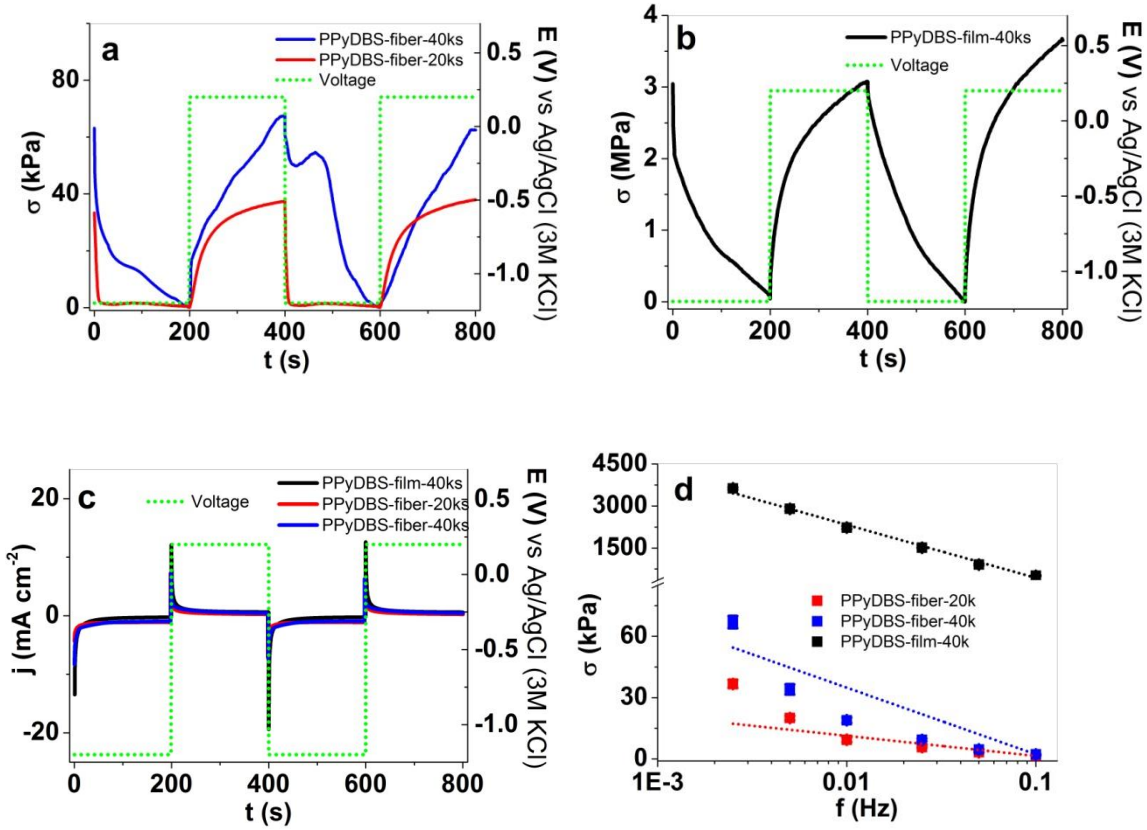

Figure 14 Square wave potentials between 0.2V to -1.2V (dotted green curve) at applied frequency 0.0025Hz (cycle 2-3) of PPyDBS-film-40ks (black), PPyDBS-fiber-20ks (red) and PPyDBS-fiber-40ks (blue) in CCM in 3 electrode cell with counter Pt sheet electrode, Ag/AgCl (3M KCl) reference electrode and the sample (1mm length constant) as working electrode. a: stress time curves of PPyDBS-fiber (40ks and 20ks), b: stress time curves of PPyDBS-film 40k, c: Current density time curve of all applied samples and d: stress σ (middle value with standard regression and linear fit) vs frequency (0.0025Hz -0.1Hz) of all samples.

The stress curves at applied frequency of 0.0025Hz for all samples (Figure 14a, b) indicate that cation-driven actuation takes place during reduction of -1.2V where the actuator expands and at oxidation the actuator contracts, comparable to Figure 14a and Figure 14b. For PPyDBS-fiber-40ks the maximum stress found is in the range of 67kPa and 36kPa for the PPyDBS-fiber-20ks. The PPyDBS-film-40ks shows stress in the range of 3MPa that relates to a pressure of 30atm. At higher frequency of up to 0.1Hz (Figure 14d) the stress decreases in nearly linear line which makes it nearly perfect behavior for the PPyDBS-film-40ks with stress at 0.1Hz of 510kPa. For the PPyDBS fibers only low stress is obtained at frequency of 0.1Hz.

PPyTF-film and -fiber scaffolds in organic electrolytes

Organic PC-TF electrolyte on PPyTF sample studies did show that if polymerized potentiostatically mixed ion movement occurred during reversible redox cycles [23], which leads to actuation at reduction and oxidation. In most cases isotonic ECMD measurements are applied and strain was determined in range of 3-7%. It was discovered that the anion $CF_3SO_3^-$ (TF) incorporate during cycling and the actuation direction changes at higher scan-rate to mainly cation-driven cycles [23]. Here we investigate galvanostatical polymerization conditions (Figure 15) of PPyTF film in free standing formation (40ks) and deposited on fiber scaffolds (40ks). The actuation properties were investigated (isometric ECMD) to determine the stress change at reversible redox reaction applying cyclic voltammetric (scan rate of 5mV/s) and square wave potential at 0.0025Hz.

Isometric ECMD response under cyclic voltammetric measurements on PPy-TF samples

Steady state condition for the PPyTF-film-40ks and PPyTF-fiber-40ks were found between 0.65V to -0.5V. Figure 15 shows the results from the isometric ECMD measurements.

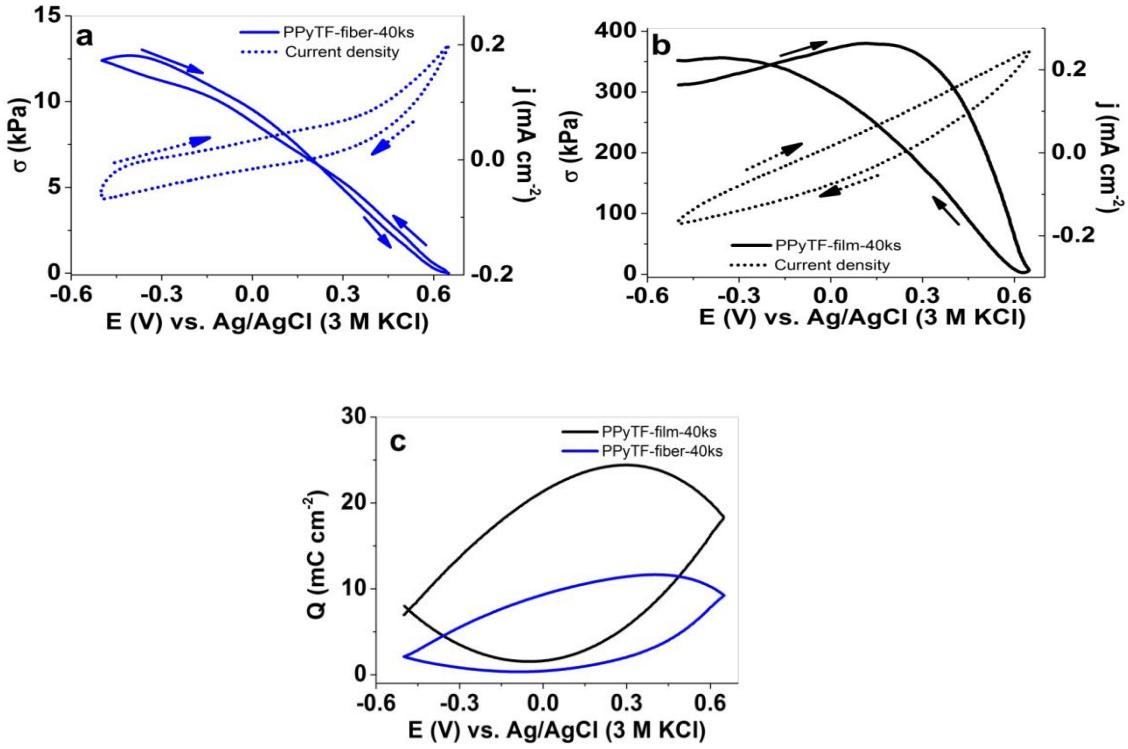

Figure 15 Cyclic voltammetric measurements (5mV/s, third cycle) under isometric ECMD control in PC-TF electrolyte of a: stress σ (kPa) potential curve of PPyTF-fiber-40ks (blue) with current density j (dotted blue curve), b: stress σ (kPa) potential curve of PPyTF-film-40ks (black) with current density j (dotted black curve) and c: charge density Q vs potential E (vs. Ag/AgCl (3M KCL reference electrode) for PPyTF-film-40ks and PPy-fiber-40ks (blue).

The PPyTF-fiber-40ks shows a stress value of 12.5kPa (Figure 15a) which direction is in opposite to PPyDBS-fiber-40ks (Figure 11a). For PPyTF samples the actuation mechanism refers to anion-driven direction with expansion at oxidation and contraction at reduction. Similar results have been shown for PPyTF free standing film in aqueous $NaPF_6$ electrolyte [23] where strain above 10% was discovered. The PPyTF-film shows stress around 350kPa with anion-driven actuation properties (Figure 15b). In comparison to PPyDBS-film in same electrolyte the stress found much higher in range of 1.5MPa (Figure 11b) but with cation-driven actuation at reversible redox cycles. The charge density (Figure 15c) reveals that the PPyTF-fiber-40ks has much lower charge density of 9.2mC cm^{-2} in comparison to PPyTF-film-40ks with 18.44mC cm^{-2}. We assume that the deposition in organic electrolyte on conductive fiber scaffolds is different from those in aqueous polymerization solution. To determine how much charge is consumed at reversible redox cycles square wave potential measurements are performed.

Isometric ECMD response at applied square wave potentials for PPyTF in PC-TF

PPyTF-fiber-40ks and PPyTF-film-40ks are investigated under isometric ECMD measurements in PC-TF electrolyte at applied potential between 0.65V to -0.5V square wave potentials are presented in Figure 16 at applied frequency of 0.0025Hz (stress vs time and current density vs time curves) and at frequency changes between 0.0025Hz up to 0.1Hz.

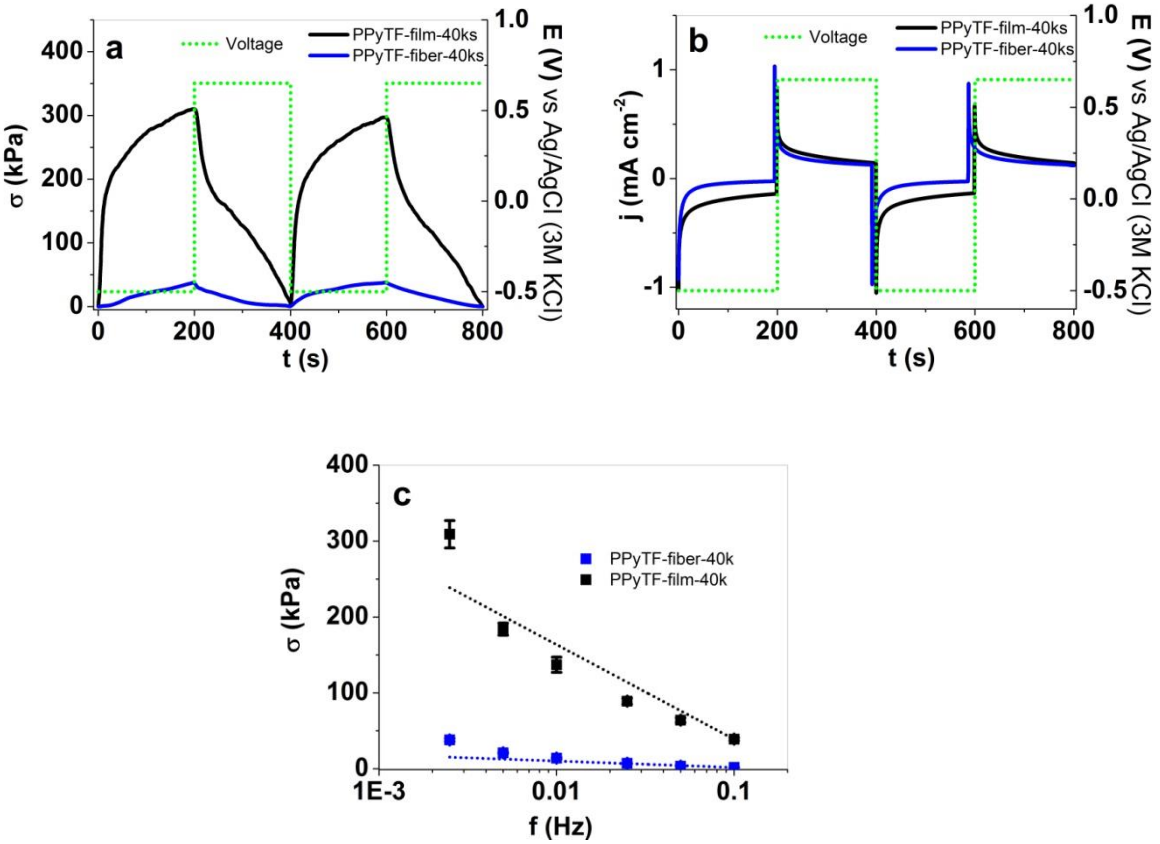

Figure 16 Square wave potentials between 0.65V to -0.5V (dotted green curve) at applied frequency of 0.0025Hz (cycle 2-3) of PPyTF-film-40ks (black) and PPyDBS-fiber-40ks (blue) in PC-TF solution in 3 electrode cell (counter Pt sheet electrode, Ag/AgCl (3M KCl) reference electrode and the sample (1 mm length constant) as working electrode). a: stress time curves, b: current density time curve and c: stress σ (middle value with standard regression and linear fit) vs frequency (0.0025Hz -0.1Hz) of all samples.

Same tendency in comparison to cyclic voltammetric ECMD response can be observed for the square wave potential measurements with PPyTF-film-40ks obtaining stress at 300kPa and for PPyTF-fiber-40ks in range of 37kPa (Figure 16a). The current densities showing for the PPyTF-film-40ks higher values (Figure 16b). The stress decreases for both samples are nearly linear with higher frequency (Figure 16c) and with much lower values in comparison to PPyDBS-film-40ks in same electrolyte (Figure 12d).

PPyTF samples in CCM

To evaluate the effect of CCM buffer on PPyTF samples isometric ECMD measurements are performed under cyclic voltammetry (5mV/s) and square wave potential (0.0025Hz) at steady state conditions in potential range of 0.3V to -0.6V.

Isometric ECMD response under cyclic voltammetric measurements on PPy-TF samples in CCM

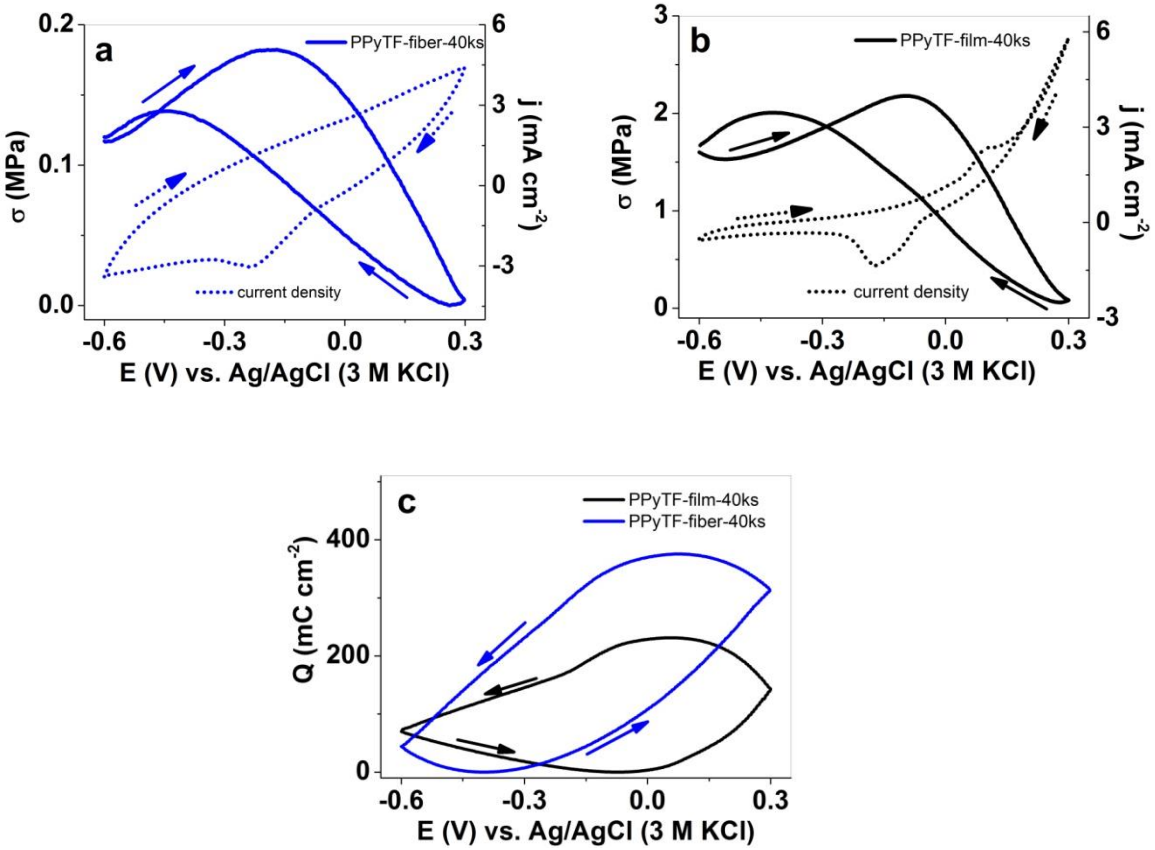

Figure 17 Cyclic voltammetric measurements (5mV/s, third cycle) under isometric ECMD control in CCM of a: stress σ (kPa) potential curve of PPyTF-fiber-40ks (blue) with current density j (dotted blue curve), b: stress σ (kPa) potential curve of PPyTF-film-40ks (black) with current density j (dotted black curve) and c: charge density Q vs potential E (vs. Ag/AgCl (3M KCL reference electrode) for PPyTF-film-40ks and PPy-fiber-40ks (blue).

The PPyTF samples in CCM buffer (Figure 17a, b) showing high stress compared to if applied in organic PC-TF electrolyte. For PPyTF-fiber-40ks (Figure 17a) stress in range of 0.18MPa was found and for PPyTF-film-40ks (Figure 17b) with mainly anion-driven actuation but also small actuation found at reduction, which hints to cation involvement. The CV shapes of both samples are showing much higher current density than observed in PPyDBS samples with correlated charge densities in the range of 311mC cm^{-2} for PPyTF-film-40ks and 142mC cm^{-2} for PPyTF-fiber-40ks. It needs to be noticed that the CV shape of PPyTF-fiber-40ks sample (Figure 17a) shows a strong reduction peak at -0.23V and for PPyTF-film-40ks (Figure 17b) the reduction peak shifts to -0.17V and an oxidation peak at 0.1V is observed. We assume that the ingredients of the CCM (DMEM, PENSTREP, FBS) contains substances that react on such

applied potential and the reaction is reflected in high charge and current density results. Nevertheless the stress values show that PPyTF-fiber-40ks gives comparable values of 0.2MPa in same electrolyte detected in PPyDBS-fiber-40ks sample (Figure 13a). The differences in both are the actuation direction from PPyDBS sample containing expansion at reduction and PPyTF sample showing expansion at oxidation.

Isometric ECMD response at applied square wave potentials for PPyTF in CCM

Square wave potentials between 0.3V and -0.6V are applied to evaluate the stress behavior (cycle2-3) at applied frequency of 0.0025Hz in PPyTF samples in CCM. The current density time curves for same frequency and the stress middle values at frequency changes from 0.0025Hz to 0.1Hz are presented in Figure 18.

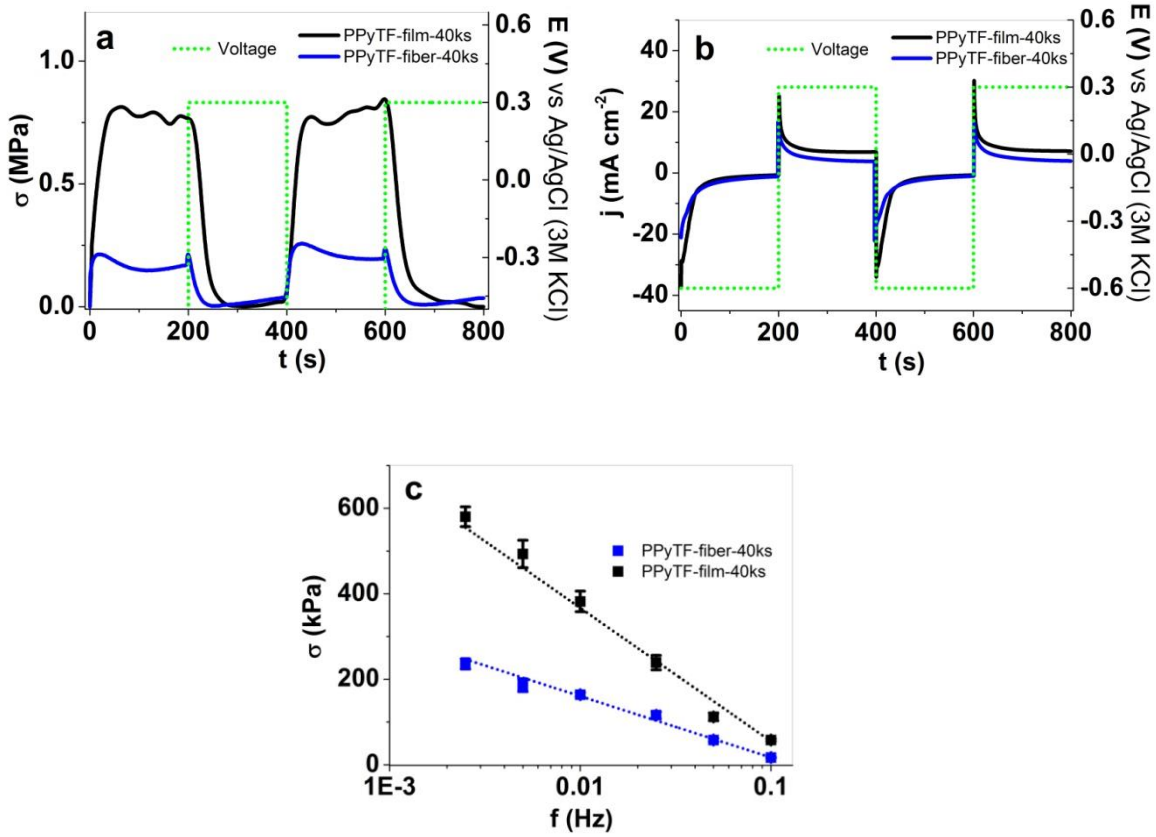

Figure 18 Square wave potentials between 0.3V to -0.6V (dotted green curve) at applied frequency of 0.0025Hz (cycle 2-3) of PPyTF-film-40ks (black) and PPyDBS-fiber-40ks (blue) in CCM in 3 electrode cell (counter Pt sheet electrode, Ag/AgCl (3M KCl) reference electrode and the sample (1 mm length constant) as working electrode)). a: stress time curves, b: current density time curve and c: stress σ (middle value with standard regression and linear fit) vs frequency (0.0025 Hz -0.1 Hz) of all samples.

Figure 18a shows stress in range of 0.8MPa for PPyTF-film-40ks and 0.2MPa for PPyTF-fiber-40ks samples. Both samples are showing expansion at oxidation and contraction at reduction

indicating mainly anion-driven actuation properties. The largest current densities measured are found in this study (Figure 18b) that we assume relies on the CCM itself. At applied frequency change of 0.0025Hz - 0.1Hz the stress decreases linearly for both samples. For the PPyTF-fiber-40ks the stress of 200 kPa is found in the CCM buffer for all investigated fiber samples. To evaluate the changes in charge densities at applied frequencies of 0.0025Hz – 0.1Hz the fiber (40ks) and film (40ks) are compared.

Comparison of PPyDBS and PPyTF samples

Square wave potential steps have been performed for the different samples at frequency range of 0.0025Hz – 0.1Hz and the stress vs charge density for PPyDBS-films and PPyTF-films in PC-TF and CCM electrolyte (Figure 19).

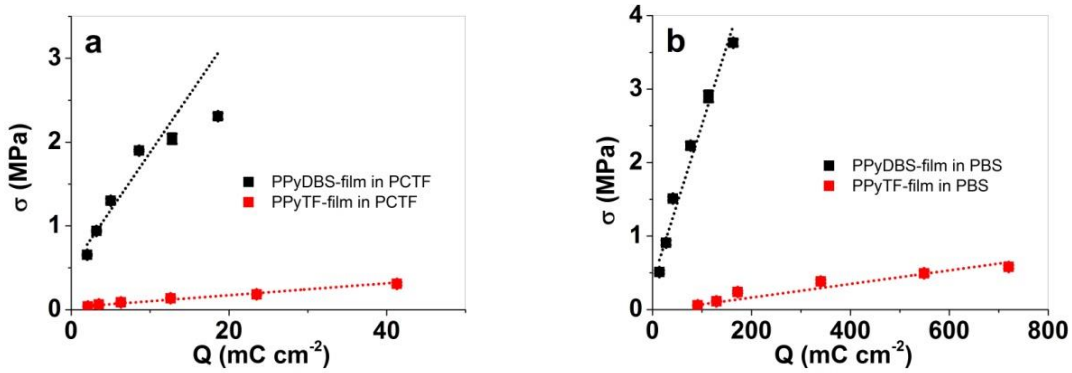

Figure 19 Stress values of PPyDBS-film (black) and PPyTF-film (red) vs. charge densities at applied frequency of 0.0025Hz – 0.1Hz in a: PC-TF electrolyte and b: CCM

The stress for PPyDBS-films in PC-TF (Figure 19a) and in CCM (Figure 19b) electrolytes are showing high stress between 0.5MPa - 4MPa with cation-driven actuation. On the other hand the PPyTF films (red) are anion-driven actuators with stress up to 0.5MPa accompanied by high charge densities in CCM solution. To investigate PPyDBS-fiber-40ks and PPyTF-fiber-40ks actuators the results are presented in Figure 20.

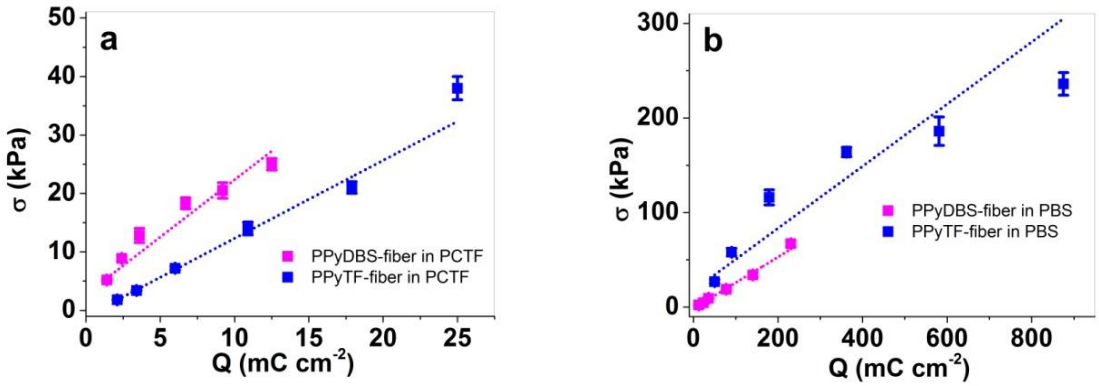

Figure 20 Stress values of PPyDBS-fiber-40ks (magneta) and PPyTF-fiber-40ks (blue) vs. charge densities at applied frequency of 0.0025Hz – 0.1Hz in a: PCTF electrolyte and b: CCM

In comparison of PPyDBS-fiber and PPyTF-fiber type the stress in PC-TF electrolyte was found in range of 30-40kPa with lower charge densities. We assume that anion-driven actuation for PPyTF-fiber in PC-TF (Figure 20a) shows higher stress because the responsible anion $CF_3SO_3^-$ is larger than the cation TBA^+ in PPyDBS-fiber (Figure 20a). In CCM solution the stress found was much higher (200kPa) with 40 times higher charge densities (Figure 20b). We assume that relies on the chosen CCM electrolyte, observed also for films (Figure 19b). Stress in range of 200kPa for PPyTF-fiber-40ks in CCM electrolyte is high enough to serve future application for mechanical STEM cell stimulation.

Summary

During this work a tri-layered electrolyte operated actuator was developed that fulfilled the goals for this thesis. Even though cell experiments were not made this material is theoretically suitable for cell and tissue experiments and stimulations.

The actuators that were developed and studied were PPy coated gelatin fiber scaffold with dodecybenzenesulfonate (DBS) or CF_3SO_3 (TF) doping. The porous structure of original fiber scaffold stayed similar after chemical deposition of PPy and also after electrochemical synthesis. After synthesis actuators were actuated in cell culture medium and propylene carbonate with 0.1M $TBACF_3SO_3$ and for reference free standing films of PPy and before mentioned dopings were actuated in same electrolytes.

The actuators were characterized by isometric electro-chemo-mechanical deformation studies with different frequencies. PPyDBS film in PC-TF and CCM showed results of 0.5MPa to 4MPa with cation driven actuation while PPyTF films were anion driven actuators and showed results up to 0.5MPa. PPyDBS and PPyTF fiber scaffolds showed results of 30kPa to 40 kPa in PC-TF with lower charge densities. In CCM PPyDBS and PPyTF fibers showed five times higher stress result and about 40 times higher charge densities than in PC-TF (Figure 20a, b).

With this thesis it was proved that PPy actuators actuated in CCM electrolyte and since the actuator itself is nontoxic and biocompatible it can be concluded that it can be used as mechano-active biointerface, for example in *vitro cell* experiments.

POLÜPÜRROOLIGA KAETUD ŽELATIINFIIBER-MATTIDE ELEKTROKEEMILIS-MEHHAANILISTE DEFORMATSIOONIDE UURINGUD

Selle töö käigus valmistati kolmekihilised elektrolüüdis aktueeruvad aktuaatorid. Kuigi rakukatseid selle töö käigus ei tehtud on valmistatud aktuaatorid teoreetiliselt rakukatseteks ja rakkude stimuleerimiseks sobivad. Töö alguses seatud eesmärgid said töö käigus kõik täidetud.

Valmistatud aktuaatorid olid polüpurrooliga kaetud želatiinist fiibermatid, millele lisati lisandiks dodetsüülbenseensulfonaati või $TBACF_3SO_3$. Fiibermattide poorne struktuur säilis ka pärast fiibrite keemilist ja elektrokeemilist katmist polüpürrooliga. Pärast polüpürrooli sünteesimist aktueeriti aktuaatoreid kahes erinevas elektrolüüdis: rakukasvu meediumis ning propüleen karbonaadis, milles oli 0.1M $TBACF_3SO_3$. Võrdluseks valmistati ka polüpürrooli kiled samade lisanditega nagu fiibermattide puhul ning neid aktueeriti samades elektrolüütides.

Aktuaatoreid karakteriseeriti isomeetrilise elektrokeemilis-mehhaanilis deformatsioonide uuringuga. Uurimistulemustest selgus, et katioonide toimel aktueerunud PPyDBS kiledes, olenevalt elektrolüüdist, mõjusid mehhaanilised pinged 0.5MPa kuni 4MPa. PPyTF kiledes, mis aktueerusid anioonide toimel, mõjusid mehhaanilised pinged kuni 0.5MPa. PPyDBS ja PPyTF fiibermattides, mida aktueeriti PC-TF elektrolüüdis, mõjusid mehhaanilised pinged 30kPa kuni 40kPa. Rakukasvu meediumis aktueeritud PPyDBS ja PPyTF fiibermatid näitasid aga 5 korda kõrgemat mehhaanilist pinget ning orienteeruvalt 40 korda paremat laengujaotust ruutsentimeetri kohta, kui PC-TF elektrolüüdis aktueeritud aktuaatorid.

Selle tööga tõestati, et valmistatud polüpürroolist aktuaatorid on võimelised ka aktueeruma rakukasvatus meediumis. Kuna valmistatud fiibermatid on ise mittetoksilised ja biosobivad, siis võib järeldada, et neid saab kasutada mehhaaniliselt aktiivsete biomaterjalidena, mida on võimalik näiteks kasutada ka rakkude stimuleerimiseks *in vitro* katsetes.

ACKNOWLEDGEMENTS

I would like to thank my supervisors, Dr. Martin Järvekülg and Dr. Rudolf Kiefer, for excellent supervision and support. In addition I would like to thank Kaido Siimon, Robert Valner, Rauno Temmer and people from IMS Lab in Tartu Technology Institute for teaching and helping me with different experiments.

REFERENCES

1. K. Siimon, P. Reemann, A. Põder, M. Pook, T. Kangur, K. Kingo, V. Jaks, U. Mäeorg, and M. Järvekülg, "Effect of glucose content on thermally cross-linked fibrous gelatin scaffolds for tissue engineering," Mater. Sci. Eng. C **42**, 538–545 (2014).

2. S.-S. Kim, J.-H. Jeon, H.-I. Kim, C. D. Kee, and I.-K. Oh, "High-Fidelity Bioelectronic Muscular Actuator Based on Graphene-Mediated and TEMPO-Oxidized Bacterial Cellulose," Adv. Funct. Mater. n/a–n/a (2015).

3. T. D. Brown, "Techniques for mechanical stimulation of cells in vitro: a review," J. Biomech. **33**, 3–14 (2000).

4. Y. Bar-Cohen, "Electroactive Polymer (EAP) Actuators as Artificial Muscles - Reality, Potential, and Challenges (2nd Edition)," .

5. K. J. Kim and S. Tadokoro, "Electroactive Polymers for Robotic Applications," .

6. R. H. Baughman, "Conducting polymer artificial muscles," Synth. Met. **78**, 339–353 (1996).

7. K. Asaka, K. Oguro, Y. Nishimura, M. Mizuhata, and H. Takenaka, "Bending of Polyelectrolyte Membrane–Platinum Composites by Electric Stimuli I. Response Characteristics to Various Waveforms," Polym. J. **27**, 436–440 (1995).

8. T. Tanaka, I. Nishio, S. T. Sun, and S. Ueno-Nishio, "Collapse of gels in an electric field.," Science **218**, 467–9 (1982).

9. R. H. Baughman, "Carbon Nanotube Actuators," Science (80-.). **284**, 1340–1344 (1999).

10. J. D. W. Madden, N. A. Vandesteeg, P. A. Anquetil, P. G. A. Madden, A. Takshi, R. Z. Pytel, S. R. Lafontaine, P. A. Wieringa, and I. W. Hunter, "Artificial Muscle Technology: Physical Principles and Naval Prospects," IEEE J. Ocean. Eng. **29**, 706–728 (2004).

11. T. F. Otero, E. Angulo, J. Rodríguez, and C. Santamaría, "Electrochemomechanical properties from a bilayer: polypyrrole / non-conducting and flexible material — artificial muscle," J. Electroanal. Chem. **341**, 369–375 (1992).

12. T. F. Otero, H. Grande, and J. Rodríguez, "A new model for electrochemical oxidation of polypyrrole under conformational relaxation control," J. Electroanal. Chem. **394**, 211–216 (1995).

13. Q. Pei and O. Inganaes, "Electrochemical applications of the bending beam method. 1. Mass transport and volume changes in polypyrrole during redox," J. Phys. Chem. **96**, 10507–10514 (1992).

14. Q. PEI and O. INGANAS, "Electrochemical applications of the bending beam method; a novel way to study ion transport in electroactive polymers," Solid State Ionics **60**, 161–166 (1993).

15. T. E. Herod and J. B. Schlenoff, "Doping-induced strain in polyaniline: stretchoelectrochemistry," Chem. Mater. **5**, 951–955 (1993).

16. L. Fan, M. Xue, Z. Kang, and S. Qiu, "Synthesis of microporous membranes and films on various substrates by novel electrospinning method," Sci. China Chem. **56**, 459–464 (2013).

17. A. Gelmi, M. K. Ljunggren, M. Rafat, and E. W. H. Jager, "Influence of conductive polymer doping on the viability of cardiac progenitor cells," J. Mater. Chem. B **2**, 3860 (2014).

18. H. Nguyen Thi Le, B. Garcia, C. Deslouis, and Q. Le Xuan, "Corrosion protection and conducting polymers: polypyrrole films on iron," Electrochim. Acta **46**, 4259–4272 (2001).

19. E. Smela, "Conjugated Polymer Actuators for Biomedical Applications," Adv. Mater. **15**, 481–494 (2003).

20. R. Kiefer, D. G. Weis, J. Travas-Sejdic, G. Urban, and J. Heinze, "Effect of electrochemical synthesis conditions on deflection of PEDOT bilayers," Sensors Actuators B Chem. **123**, 379–383 (2007).

21. S. Maw, E. Smela, K. Yoshida, P. Sommer-Larsen, and R. B. Stein, "The effects of varying deposition current density on bending behaviour in PPy(DBS)-actuated bending beams," Sensors Actuators A Phys. **89**, 175–184 (2001).

22. N. Aydemir, P. A. Kilmartin, J. Travas-Sejdic, A. Kesküla, A.-L. Peikolainen, J. Parcell, M. Harjo, A. Aabloo, and R. Kiefer, "Electrolyte and solvent effects in PPy/DBS linear actuators," Sensors Actuators B Chem. **216**, 24–32 (2015).

23. R. Kiefer, S. Y. Chu, P. A. Kilmartin, G. A. Bowmaker, R. P. Cooney, and J. Travas-Sejdic, "Mixed-ion linear actuation behaviour of polypyrrole," Electrochim. Acta **52**, 2386–2391 (2007).

24. S. Y. Chu, P. A. Kilmartin, and J. Travas-Sejdic, "Effects of applied stress and long-term stability on PPy(CF3SO3) linear actuators," Synth. Met. **159**, 2286–2288 (2009).

25. R. Stankoviç, O. Pavloviç, M. Vojnoviç, and S. Jovanoviç, "The effects of preparation conditions on the properties of electrochemically synthesized thick films of polypyrrole," Eur. Polym. J. **30**, 385–393 (1994).

26. A. Kaynak, "Effect of synthesis parameters on the surface morphology of conducting polypyrrole films," Mater. Res. Bull. **32**, 271–285 (1997).

27. R. Temmer, I. Must, F. Kaasik, A. Aabloo, and T. Tamm, "Combined chemical and electrochemical synthesis methods for metal-free polypyrrole actuators," Sensors Actuators B Chem. **166-167**, 411–418 (2012).

28. L. Valero, T. F. Otero, and J. G. Martínez, "Exchanged cations and water during reactions in polypyrrole macroions from artificial muscles.," Chemphyschem **15**, 293–301 (2014).

29. K. Siimon, H. Siimon, and M. Järvekülg, "Mechanical characterization of electrospun gelatin scaffolds cross-linked by glucose.," J. Mater. Sci. Mater. Med. **26**, 5375 (2015).

30. R. Temmer, "Elecrochemistry and novel applications of chemically synthesized conductive polymer electrodes."

LIHTLITSENTS

Mina, Madis Harjo

1. Annan Tartu Ülikoolile tasuta loa (lihtlitsentsi) enda loodud teose

“ Electro-chemo-mechanical deformation studies on polypyrrole covered gelatin fiber scaffolds”

mille juhendajad on Rudolf Kiefer ja Martin järvekülg

(a) Reprodutseerimiseks säilitamise ja üldsusele kättesaadavaks tegemise eesmärgil, seal hulgas digitaalarhiiv Dspace’is lisamise eesmärgil kuni autoriõiguse kehtivuse tähtaja lõppemiseni;

(b) Üldsusele kättesaadavaks tegemiseks Tartu Ülikooli veebikeskkonna kaudu, sealhulgas digitaalarhiivi DSpace’i kaudu kuni autoriõiguse kehtivuse tähtaja lõppemiseni.

2. Olen teadlik, et punktis 1 nimetatud õigused jäävad alles ka autorile;

3. Kinnitan, et lihtlitsentsi andmisega ei rikuta teiste isikute intellektuaalomandi ega isikuandmete kaitse seadusest tulenevaid õigusi.

Tartus, 31.05.2016